JMEPEG (2009) 18:966–972
DOI: 10.1007/s11665-008-9315-4

1059-9495/$19.00

Deformation Behavior of AZ31 Magnesium Alloy During Tension at Moderate Temperatures

Junwei Liu, Ding Chen, Zhenhua Chen, and Hongge Yan

(Submitted April 19, 2008; in revised form September 7, 2008)

The mechanical properties and deformation mechanisms have been studied by tension testing at temperatures between 373 and 523 K and at strain rates ranging from 10^{-1} to 10^{-3} s^{-1}. The experimental results show that the plasticity improves significantly with temperature and decreases obviously with increasing strain rate. When the temperature is below the recrystallization temperature, twinning and dislocation slip have been proven to be the dominant model of plastic deformation. With the temperature increasing, some DRXed grains can be observed at the twinned regions and grain boundaries, suggesting that both twinning-induced DRX and continuous DRX occurred in the deformation process.

Keywords dislocation slip, magnesium alloy, tension, twinning

1. Introduction

As the currently lightest alloys used as structural metals, magnesium (Mg) alloys are being increasingly used in electronics, automobile, and aerospace industries (Ref 1-3). Up to now, production of Mg alloys has been almost entirely in the field of pressure die casting because of its high productivity and dimensional accuracy. However, due to the *hcp* structure and low stacking fault energy (SFE) of Mg, the accommodating ability and ductility of Mg alloys at moderate temperatures are rather poor. Because of common sharp crystallographic textures in wrought product, especially for metals with *hcp* structure, AZ31 Mg alloys exhibit special deformation properties in ambient and moderate temperatures (Ref 4). For these reasons, the large scale utilization of sheet-formed Mg alloys, e.g., AZ31 Mg alloy sheet, has not developed.

Yin et al. (Ref 5) has carefully investigated the relationship between dynamic recrystallization (DRX) and twinning, and then suggested a twinning-induced DRX model at a temperature range of 323-473 K. By examining the deformation properties of hot-rolled AZ31 Mg alloys, they found that with the increase of the internal stress up to the critical resolved shear stress (CRSS) for activation of nonbasal slip, the dislocation pile up and three-dimensional DRX nuclei are formed by the interaction between a and $a + c$ dislocations. Jiang et al. (Ref 6) pointed out that {10-11} contraction twins-induced softening overrides both the twinning-induced hardening and dislocation hardening in polycrystalline AM30 Mg alloy at moderate temperatures (398-623 K). However, the systematic research on the microstructure evolution and mechanical properties for hot-rolled Mg alloy sheets were not mentioned. The heterogeneous combination of slip, twinning, and DRX is still unconfirmed at moderate temperatures.

For this purpose, uniaxial tension tests of typical rolled AZ31 Mg alloys were utilized to evaluate the deformation behaviors at a range of moderate temperatures (373-523 K) in this study. By using optical microscopy (OM), high-resolution transmission electron microscopy (HRTEM), and scanning electronic microscopy (SEM), the relationship of slip, twinning, and DRX in deformation process is analyzed.

Junwei Liu, Ding Chen, Zhenhua Chen, and **Hongge Yan**, College of Materials Science and Engineering, Hunan University, Changsha 410082, China. Contact e-mail: liujw1981@hotmail.com.

2. Experimental

2.1 Experimental Materials

The as-received AZ31 billet (160 mm diameter × 300 mm high) used in this study were obtained from Ruige Ltd., Shanxi, China. The chemical composition of used AZ31 Mg alloy is presented in Table 1. After extrusion (extrusion ratio 17.8:1), the Mg alloy blocks with a thickness of 7.5 mm were cut from the extruded Mg alloy sheet.

Before rolling, the roller was lubricated by graphite and the blocks were heated at 673 K for 1800 s. Then the blocks were subjected to first rolling pass of 10% reduction (calculated with evolution of thickness) at 573 K (two high configuration, 150 mm diameter × 190 mm wide rolls, rolling speed: 0.43 m/s). A larger thickness reduction in the first pass caused cracking although larger reductions can be imposed in the following pass. The rolls were then heated to 573 K prior to repeat rolling. Specimens were then immediately rolled 9 passes of 16% reduction per pass. The specimens were air cooled after the final pass and, finally, the blocks were rolled to a thickness of 1.1 mm. Tensile specimens were prepared using electrical-discharge machining from the rolled sheets with their tensile axes parallel to the rolled direction. The tensile specimens had a gage Sect. 15 mm long and 4 mm wide, as shown in Fig. 1.

2.2 Experimental Procedure

Tension tests were carried out using a computer servo-controlled Gleeble 1500 machine to examine the warm

deformation properties of AZ31 Mg alloy at a temperature range of 373-523 K and a strain rate range of 10^{-3}-10^{-1} s^{-1}. Prior to tensile testing, the furnace was heated to the test temperature and the specimen was then inserted into the tensile grips. The specimen was allowed to heat up and stabilize at the desired temperature (total time: 10-15 min) before pulling to fracture, after which it was immediately removed from the furnace and quenched in water. X-ray texture analysis was carried out in the rolled samples using the Schule reflection method in a Siemens D500 diffractometer furnished with a closed Eulerian cradle. The deformed microstructures sectioned parallel to the deformation axis were observed using an MM-6 metallographic microscope. Specimens were prepared using standard metallographic techniques, finishing with 1 μm diamond paste in methanol. Acetic picral solution (5 g picric acid, 10 mL water, 5 mL acetic acid, and 90 mL ethanol) was employed to etch the specimens for 5-10 s. A JEM-3010 HRTEM at 200 kV was used for the morphology observation. HRTEM specimens which are parallel to the applied stress axis were cutoff from the samples followed by mechanical grinding to 0.03-0.05 mm. Then the slices were thinned by conventional twin jet polishing technique using an electrolyte consisting of 5% $HClO_4$, 35% butanol, and 60% methanol at 243 K. To examine certain features of the fractured surfaces in more detail, electronic microscopy was performed using PHILIPS SEM515.

3. Results and Discussion

3.1 Mechanical Behaviors

Figures 2 and 3 are summaries of mechanical properties of rolled AZ31 Mg alloy in the current study. The values of true stress and true strain can be calculated by the following equations:

$$\sigma_T = \sigma_{eng}\left(\frac{l_0 + l}{l_0}\right) \quad \text{(Eq 1)}$$

Table 1 Chemical composition (in wt.%) of the hot-rolled AZ31 alloy

Al	Zn	Mn	Fe	Cu	Ca	Mg
3.13	0.87	0.44	0.002max	0.1max	0.03max	Balanced

$$\sigma_{eng} = \frac{P_t}{A_0} \quad \text{(Eq 2)}$$

$$\varepsilon_T = \ln\left(\frac{l_0 + l}{l_0}\right) \quad \text{(Eq 3)}$$

where σ_T represents the true stress, σ_{eng} is the engineering stress, l_0 is gage length, l is percentage elongation, P_t is the load in the deformation processing, A_0 is the initial transversal superficial measure of the sample, and ε_T is the true strain.

From Fig. 2 and 3, it is shown that the ductility in tension increases with deformation temperature and decreases with increasing strain rate, showing obvious strain rate sensitivity. In Fig. 2, fracture at strain ε_f precedes or shortly follows the peak of the curve at low temperatures. Above 473 K, the peaks are followed by work softening with approach to a steady-state appearing only at higher *T*. Peak stress is generally accepted to be the equilibrium point caused by the hardening and softening; therefore, the softening mechanisms, such as DRX, dislocation slip, and twinning, actually occurs before peak stress (Ref 5). Meanwhile, it can also be observed from Fig. 3 that peak stress decreases sharply with increasing strain rates, further suggesting that the flow stress behavior depends on the strain rate. This is because that the nucleation rate and growth velocity of dislocation is insensitive to strain rate, compared to twinning. Therefore, in the deformation process with high strain rates, a small amount of gissile dislocations can not effectively release the stress concentration and retard failure.

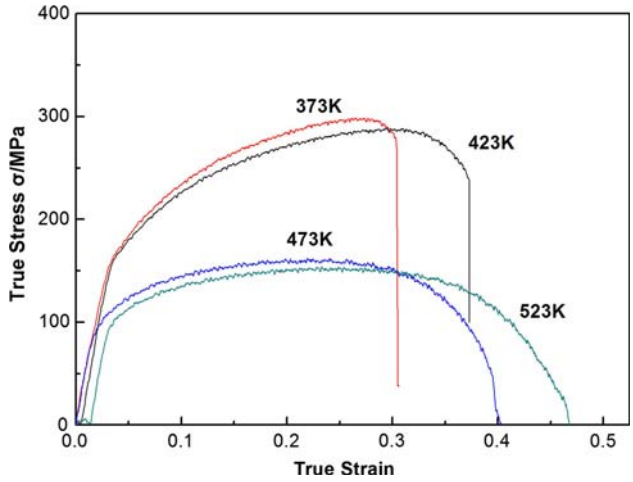

Fig. 2 Flow curves obtained at 0.5×10^{-2} s^{-1} and various temperatures

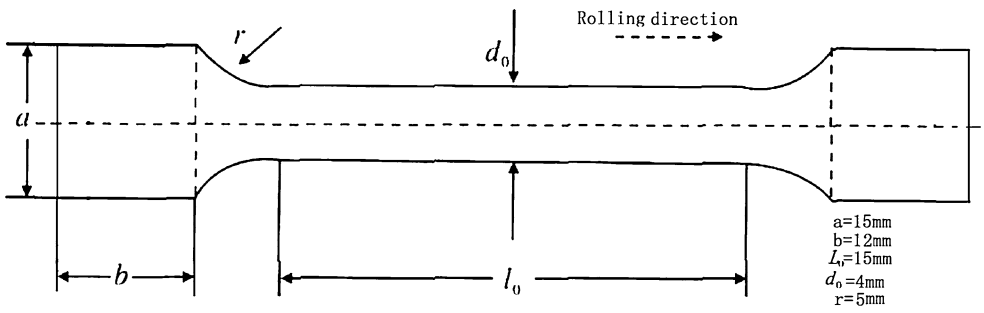

Fig. 1 Schematic overview of the configuration of the AZ31 Mg alloy tensile sample

In Mg alloys, basal slip, $a + c$ nonbasal slip, twinning, and DRX are the four major mechanisms involved in the release of stress (Ref 7, 8). At temperatures below those at which individual atoms are mobile, slip and twinning are the major deformation modes which enable a solid to change shape under the action of an applied stress. However, the activation of pyramidal and prismatic slip systems in Mg alloy aggregates occurs primarily due to the large stresses generated in grain-boundary regions because of misorientation between neighboring grains. So the critical resolved shear stress (CRSS) of pyramidal and prismatic slip is difficult to be surpassed and there were few slip systems activated during deformation processing.

As reported, CRSS for a basal slip system is much lower than those of nonbasal slip systems on pyramidal planes, as well as the twinning modes (Ref 7-10). For the present hot-rolled samples which have a strong basal plane texture (Fig. 4),

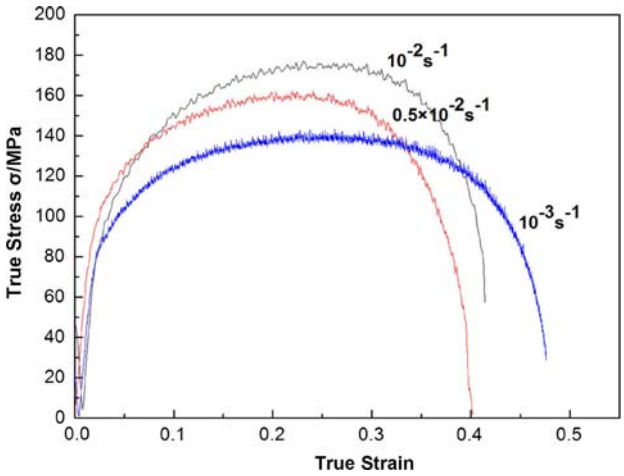

Fig. 3 Flow curves obtained at 473 K and various strain rates

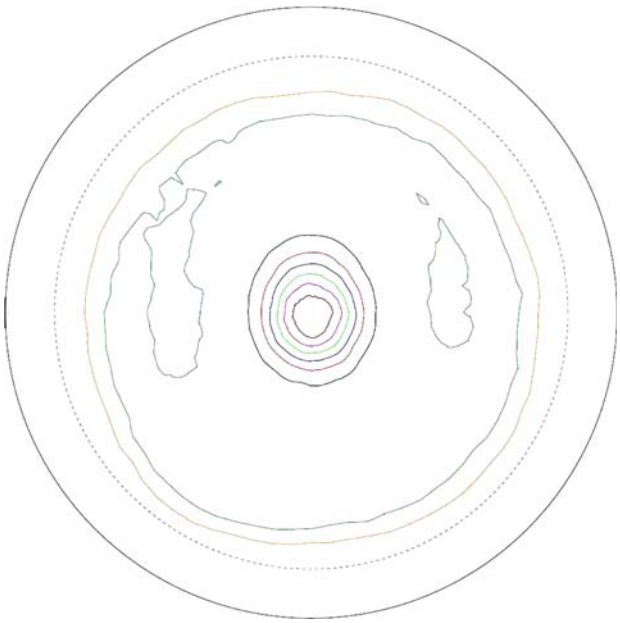

Fig. 4 Macrotexture of the rolled sample illustrated using (0002) pole figure

stress direction is nearly parallel to the basal plane. Because of the small orientation factor, which denotes a extremely low shear stress on the basal slip system, the basal slip is limited in the tensile loading conditions. However, the CRSS for basal slip is only 2 MPa in AZ31 Mg alloy. Thereby, a slight misalignment (about 10°) of basal plane can induce the operation of basal slip (Ref 9, 10). By these reasons, on the one hand, softening mechanisms of Mg alloys are often exhibited by twinning and basal slip, when the temperature is below recrystallization temperature.

On the other hand, with the temperature increasing and reaching recrystallization temperature, CRSS for nonbasal slip declines with an increase in temperature and a great amount of dislocations are prone to expand at their slip planes and form dislocation networks with high density of tangled dislocations. According to Basinski mechanism, these tangled dislocations are difficult to free from these networks, consequently the dominant softening mechanisms of Mg alloys are DRX and twinning.

3.2 Microstructure Evolution

The microstructure of samples strained to failure at 423 K at different strain rates are illustrated in Fig. 5. It is evident that the amount of twinning increases significantly with strain rate. It is known that there are two types of twins frequently reported in alloys: delayed twinning (common in *fcc* metals) which usually has a rather small effect on the actual stress versus strain curve and immediate twinning (common in *hcp* metals) which is often characterized by very rapid formation of twinned regions (Ref 11). Twinning of this latter type is very sensitive to temperature of deformation and to strain rate, the relative contribution of twinning to overall strain increases as the temperature is lowered or the strain rate is increased. By this reason, the amount of twinning decreases with increasing temperature, as presented in Fig. 6.

In Fig. 6(a) and (b), although the amount of twins is not too much, twinning is obviously visible in these "big" grains. It is clear that the nucleation and growth of twins is improbable unless there is a combination of very high stress and strain energies. There are two reasons to explain the phenomenon that twins only appear in coarse grains: (1) Fine grains can not provide high stress concentration; (2) the boundary of these fine grains also restrict the growth of twins (Ref 11, 12). As shown in Fig. 5(c) and 6(c), twins occurred in parallel bundles, mainly quite narrow and sometimes encroaching on each other laterally. This is because that in any one matrix grain there are as many as six twinning planes. Due to the six planes available for a type of twinning, there are further misorientation relationships possible between the twins themselves as shown in Table 2. Moreover, three types of twins are reported in Mg alloys: extension twins, contraction twins, and double twins. In some cases, these different types of twins could intersect with each other and result in severe shear in the existing twin. In other cases, the more recently formed twins simply stopped at the older one.

Figure 7 shows typical microstructures of the hot-rolled AZ31 alloy deformed at 523 K. From Fig. 7, it is clear that tiny grains of about 1-2 μm begin to nucleate structures and entire microstructure become extremely inhomogeneous. It can be concluded that some of the grains are very sensitive to DRX, and thus are quickly replaced by DRXed grains, while some grains are present which are insensitive to DRX. As can be seen

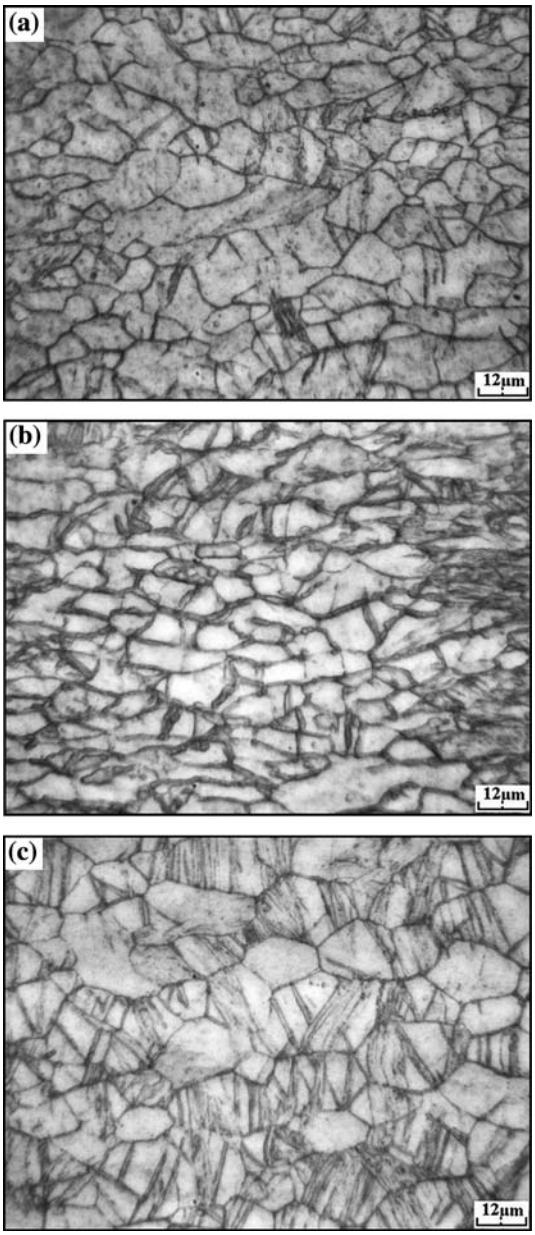

Fig. 5 Microstructures obtained at 423 K and various strain rates: (a) 10^{-3} s^{-1}, (b) 0.5×10^{-2} s^{-1}, and (c) 10^{-2} s^{-1}

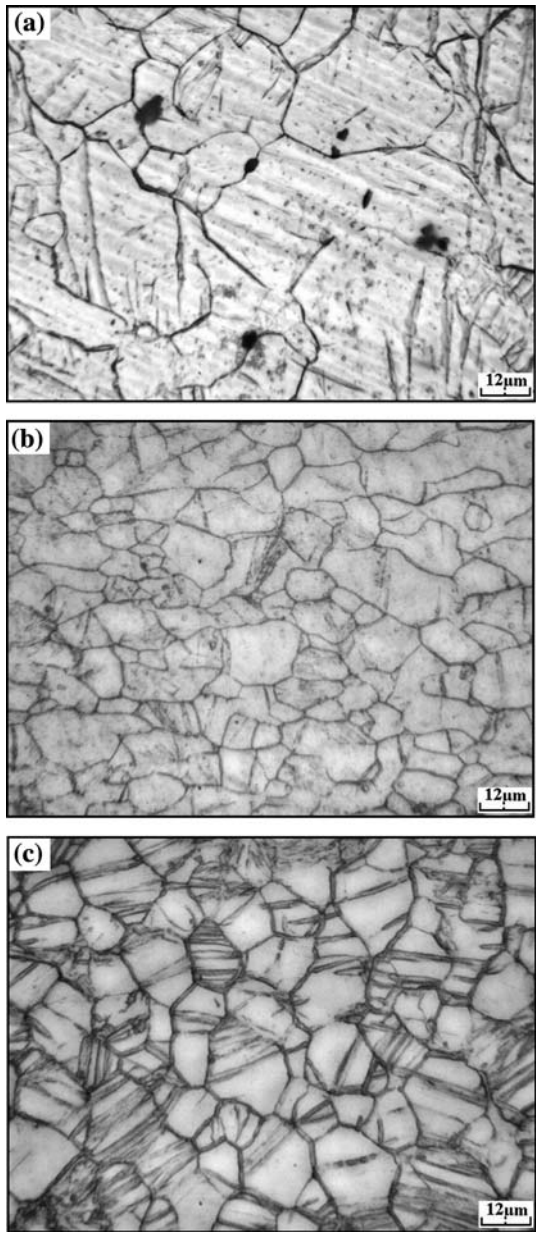

Fig. 6 Microstructures obtained at 0.5×10^{-2} s^{-1} and various temperatures: (a) 473 K, (b) 423 K, and (c) 373 K

in Fig. 7(a), there is a large uncrystallized grain, while the surrounding area of this large grain has already been replaced by fine grains (as indicated by Region A in Fig. 7a, b). The uneven rate of recrystallization at different grains is considered to be the main reason for the inhomogeneous microstructure. Moreover, DRXed grains can be occasionally observed at the twinned regions (as indicated by the Region B in Fig. 7a-c). It is often observed that the size of DRXed grains can be estimated by the width of the twins, suggesting that the nucleation of DRXed grains is closely related to the specific mechanism associated with the twinning.

In fact, the most commonly observed DRX mechanisms in Mg alloy are twinning-induced DRX and continuous DRX. Continuous DRX which is characterized by direct transformation of subgrains into high-angle grains is believed to be the predominant mechanism for the nucleation of new grains in Mg alloys (Ref 13). For twinning-induced DRX, basal dislocations accumulate near twin boundaries in the initial stage of twinning. With the continuous deformation, the dislocation pile-up and stress concentration become serious, which increases the internal stress up to the CRSS for the activation of $a + c$ nonbasal slip. Therefore, nonbasal slips are activated near grain boundary and three-dimensional DRX nuclei are

Table 2 Misorientation relationships between various {10-11} twin variants

Type of twin	Misorientation angle, °
(10-11)-(-1011)	56.1
(10-11)-(0-111)	80.3
(10-11)-(1-101)	52.4

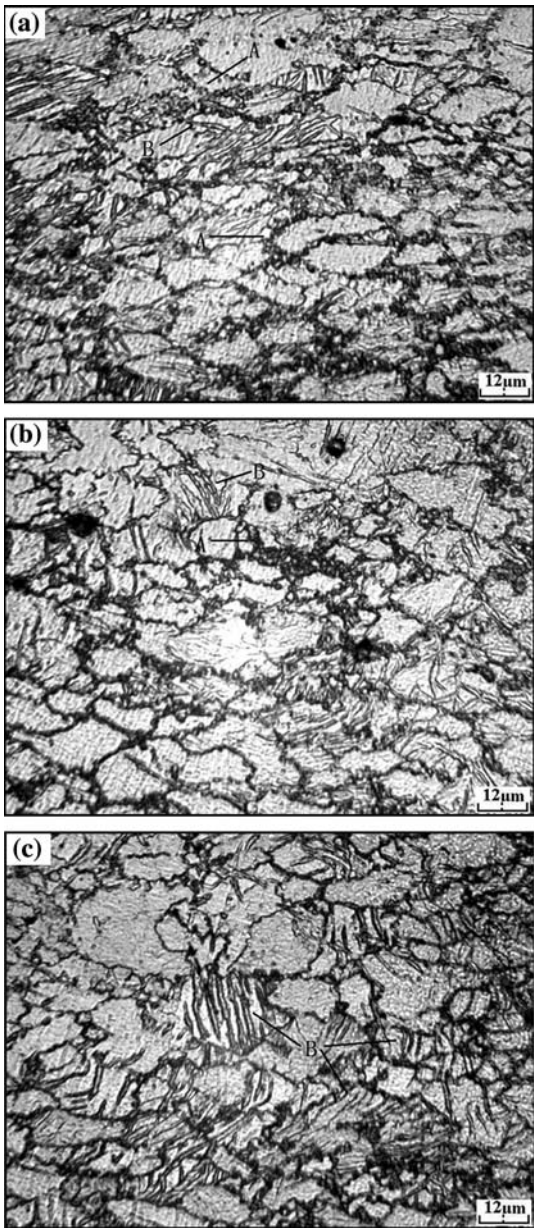

Fig. 7 Microstructures obtained at 523 K and various strain rates: (a) 0.5×10^{-2} s^{-1}, (b) 10^{-2} s^{-1}, and (c) 10^{-3} s^{-1}

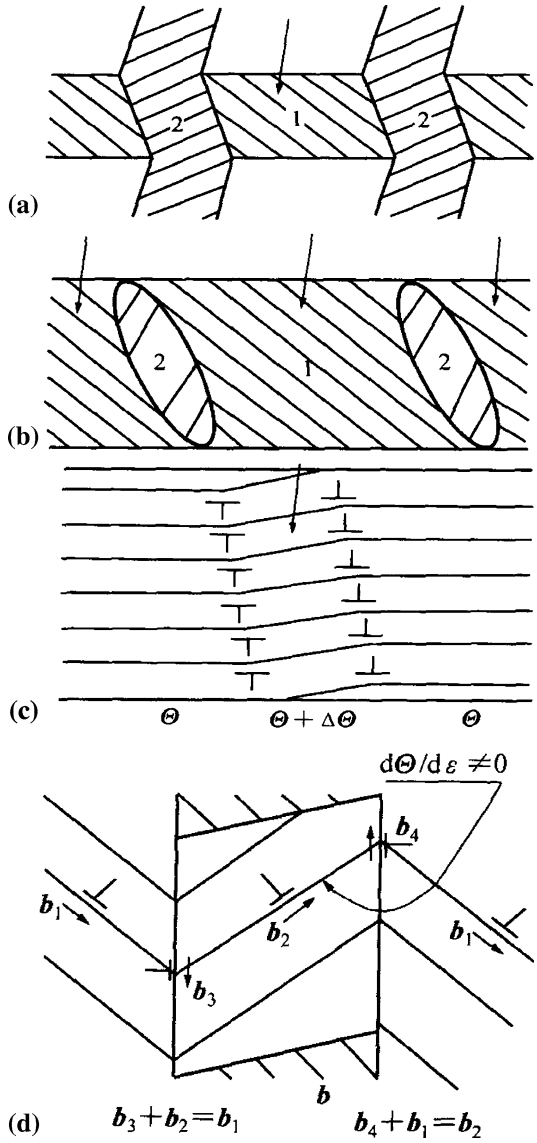

Fig. 8 Schematic representation of TDRX mechanism: (a) Mutual intersection of primary twins 1 and 2; (b) Subdivision of coarse primary twin lamellas 1 by fine secondary twins 2; (c) Subdivision of primary twin lamellas by transverse low-angle boundaries; and (d) Scheme of formation of orientation misfit dislocations (with Burger vectors $\boldsymbol{b}_3$ and $\boldsymbol{b}_4$) in twin boundaries providing a change in misorientation of twin boundaries

formed by the interaction between a and $a + c$ dislocations. Otherwise, the intersection of different types of twins also leads to the occurrence of DRXed grains, as shown in Fig 8. By passing through low-angle boundaries, primary twin lamellas were divided. Under the control of grain boundary migration (GBM), the DRX nuclei grow to recrystallized small grains (Ref 14).

3.3 HRTEM Image

Figure 9 presents typical HRTEM micrographs showing the deformation twins. From these images, it is obvious that twins occurred in parallel bundles and the average size, in width, is only 40-300 nm.

As shown in Fig. 9(a) and (b), another feature of the microstructure is the dislocation arrays that can be observed in the top and bottom of twin plates. Some of the dislocation arrays also existed in the twin plate. As mentioned before, dislocation slip contributes to the plastic deformation, besides twinning. Dislocations in the top and bottom of twin plates form dislocation network; this further confirmed that dislocations are not only more on basal planes, but also slip on prismatic and pyramidal planes in Mg alloy. Normally, a high density of dislocations may cause changes to crystal orientations and eventually become grain boundaries. Previous work has pointed out that a sufficient number of dislocations could induce the formations of grains with different orientations (Ref 11-13). However, due to the limitation of recrystallization temperature and strain energy, the dislocation arrays in twin plate only subdivide the twin platelets into smaller parts that have less different orientations.

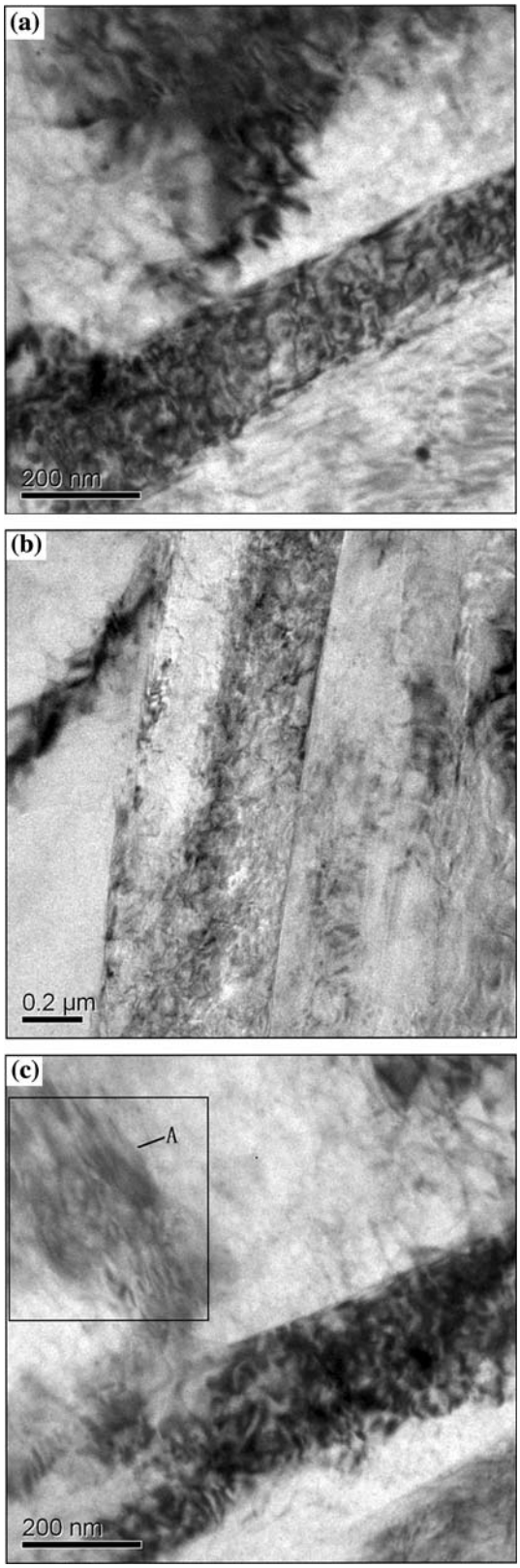

Fig. 9 HRTEM images of specimens elongated at different conditions: (a, b) 423 K, 10^{-1} s^{-1} and (c) 523 K, 10^{-2} s^{-1}

Figure 9(c) is a typical example of freshly formed clean new grains in the heavily deformed twin platelet near the twin interface. From Fig. 9(c), the originally large grains or platelets start being divided into smaller grains (Region A in Fig. 9c) through DRX, implying that the distortion energy accumulated by twinning in the initial stage of deformation is the reason for nucleation of DRX in the immediate stage of deformation.

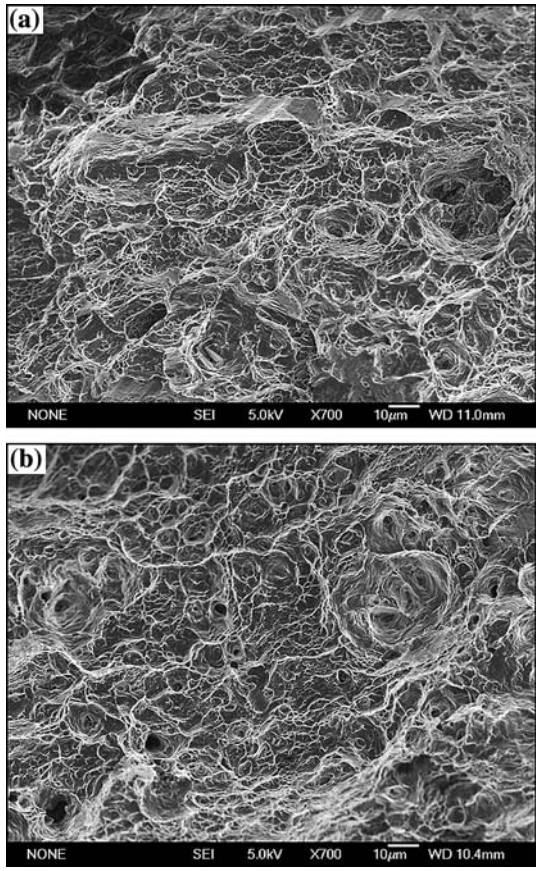

Fig. 10 SEM fractography of hot-rolled AZ31 at different conditions: (a) 373 K, 10^{-2} s^{-1} and (b) 623 K, 10^{-2} s^{-1}

3.4 SEM Image

Figure 10 illustrates SEM fractography of AZ31 Mg alloy deformed at different conditions. The fracture surface in Fig. 10(a) consists of some dimples and a few cleavage facets. The fracture manner basically belongs to the combination of ductile and brittle fracture. With the temperature increasing, it is clearly observed from Fig. 10(b) that fracture surface of AZ31 Mg alloy deformed at 10^{-2} s^{-1} and 423 K have obvious dimple characteristic and their mechanism turned into ductile fracture. Some of the dimples distribute unevenly among the tearing edges with transverse size ranging from 5 to 15 μm.

4. Conclusions

The deformation behavior of AZ31 Mg alloy during tension at moderate temperatures has been studied. Conclusions from the present work can be summarized by the following:

1. With the increasing strain rate and decreasing temperature, the peak stress of the alloy increases remarkably, while the elongation of the alloy decreases greatly, showing obvious strain rate sensitivity.

2. When the temperature is below the recrystallization temperature, twinning and dislocation slip, including basal slip and $a + c$ nonbasal slip, have been proven to be the dominant model of plastic deformation. With the temperature increasing, obvious DRX occurs in deformation process.
3. The main DRX mechanism of AZ31 under the investigated conditions is the conventional continuous DRX. These DRX grains nucleate by bulging of some portions of serrated grain boundaries. However, some of the DRXed grains are continuously nucleated in the twinned regions, suggesting that the nucleation of these DRXed grains is closely related to twinning-induced DRX.
4. Fracture observation shows that with the temperature increasing, the fracture mechanism changes from mixture of ductile and brittle fracture with some cleavage facets to ductile fracture with many dimples.

References

1. A. Jager, P. Lukac, V. Gartnerova, J. Haloda, and M. Dopita, Influence of Annealing on the Microstructure of Commercial Mg Alloy AZ31 After Mechanical Forming, *Mater. Sci. Eng. A*, 2006, **432**, p 20–25
2. Q. Guo, H.G. Yan, H. Zhang, Z.H. Chen, and Z.F. Wang, Behaviour of AZ31 Magnesium Alloy During Compression at Elevated Temperatures, *Mater. Sci. Technol.*, 2005, **21**, p 1349–1354
3. T. Mohri, M. Mabuchi, N. Nakamura, T. Asahina, H. Iwasaki, T. Aizawa, and K. Higashi, Microstructural Evolution and Superplasticity of Rolled Mg-9Al-1Zn, *Mater. Sci. Eng. A*, 2000, **290**, p 139
4. M.R. Barnett, M.D. Nave, and C.J. Battles, Deformation Microstructures and Textures of Some Cold Rolled Mg Alloys, *Scr. Mater.*, 2004, **51**, p 881–885
5. D.L. Yin, K.F. Zhang, G.F. Wang, and W.B. Han, Warm Deformation Behavior of Hot-Rolled AZ31 Mg Alloy, *Mater. Sci. Eng. A*, 2005, **392**, p 320–325
6. L. Jiang, J.J. Jonas, A.A. Luo, A.K. Sachdev, and S. Godet, Influence of {10-12} Extension Twinning on the Flow Behavior of AZ31 Mg Alloy, *Mater. Sci. Eng. A*, 2007, **445–446**, p 302–309
7. H.Q. Sun, Y.N. Shi, M.X. Zhang, and K. Lu, Plastic Strain-Induced Grain Refinement in the Nanometer Scale in a Mg Alloy, *Acta Mater.*, 2007, **55**, p 975–982
8. S.G. Tian, L. Wang, K.Y. Sohn, K.H. Kim, Y.B. Xu, and Z.Q. Hu, Microstructure Evolution and Deformation Features of AZ31 Mg-Alloy During Creep, *Mater. Sci. Eng. A*, 2006, **415**, p 309–316
9. L. Jiang, J.J. Jonas, A.A. Luo, A.K. Sachdev, and S. Godet, Twinning-Induced Softening in Polycrystalline AM30Mg Alloy at Moderate Temperatures, *Scr. Mater.*, 2006, **54**, p 771–775
10. Y.N. Wang and J.C. Huang, The Role of Twinning and Untwinning in Yielding Behavior in Hot-Extruded Mg–Al–Zn Alloy, *Acta Mater.*, 2007, **55**, p 897–905
11. J.W. Christian and S. Mahajan, Deformation Twinning, *Prog. Mater. Sci.*, 1995, **39**, p 1–157
12. M.R. Barrnett, Twinning and Ductility of Magnesium Alloys Part II. "Contract Twins", *Mater. Sci. Eng. A*, 2007, **464**, p 8–16
13. Q.L. Jin, S.Y. Shim, and S.G. Lim, Correlation of Microstructural Evolution and Formation of Basal Texture in a Coarse Grained Mg–Al Alloy During Hot Rolling, *Scr. Mater.*, 2006, **55**, p 843–846
14. M.M. Myshlyaev, H.J. Mcqueen, A. Mwembela, and E. Konopleva, Twinning, dynamic recovery and recrystallization in hot worked Mg–Al–Zn alloy, *Mater. Sci. Eng. A*, 2002, **337**, p 121–133